Revision of the Standard Hydrodynamic Transport Model for SOI Simulation

Markus Gritsch, Hans Kosina, *Member, IEEE*, Tibor Grasser, and Siegfried Selberherr, *Fellow, IEEE*

***Abstract*—Anomalous output characteristics are observed in hydrodynamic simulations of partially depleted SOI MOSFETs. The effect that the drain current reaches a maximum and then decreases is peculiar to the hydrodynamic transport model. It is not observed in drift-diffusion simulations and its occurance in measurements is questionable. An explanation of the cause of this effect is given and a solution is proposed by modifying the hydrodynamic transport model.**

***Index Terms*—Device simulation, hydrodynamic transport model, numerical analysis, semiconductor device modeling, SOI MOSFET.**

I. INTRODUCTION

USING the standard hydrodynamic (HD) transport model for simulation of partially depleted SOI MOSFETs, an anomalous decrease of the drain current with increasing drain–source voltage has been observed (Fig. 1).

The anomalous effect has been reproduced using the two different device simulators MINIMOS-NT [1] and DESSIS [2] and can be explained by an enhanced diffusion of channel hot carriers into the floating body [3], [4]. It is believed that this decrease in drain current is an artifact because experimental data do not show this effect, nor can it be observed when using the drift-diffusion (DD) transport model. One exception is given in [5], where a weak decrease of the measured drain current of a p-MOS SOI is reported.

However, applicability of the HD model to the ever downscaled devices is desirable, because in contrast to the DD model it takes nonlocal effects into account. Empirical measures provided by DESSIS, such as weighting heat flow and thermal diffusion, have only little influence on the current drop. It is assumed that the anomalous current drop is a consequence of several physical assumptions usually made in the derivation of the standard HD model. We present a modified HD model, which accounts for an anisotropic carrier temperature and a non-Maxwellian distribution function. This new model is implemented in MINIMOS-NT and gives proper results for partially depleted SOI MOSFETs. The additional model parameters are estimated from Monte-Carlo (MC) calculations.

Manuscript received April 4, 2002; revised July 8, 2002. This work was supported in part by Intel Corp., Santa Clara, CA and by the Christian Doppler Forschungsgesellschaft, Vienna, Austria. The review of this paper was arranged by Editor P. Yang.

The authors are with the Institute for Microelectronics, Technical University of Vienna, A-1040 Vienna, Austria (e-mail: gritsch@iue.tuwien.ac.at).

Publisher Item Identifier 10.1109/TED.2002.803645.

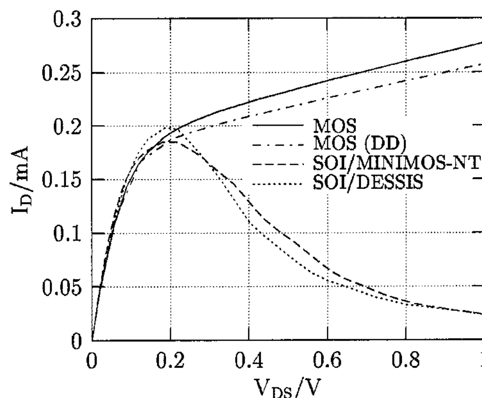

Fig. 1. Output characteristics obtained by standard DD and HD simulations verified by using two different device simulators.

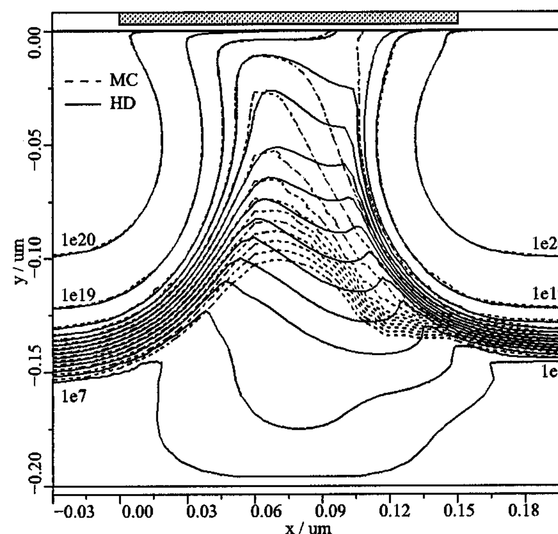

Fig. 2. Electron concentration in an SOI MOSFET obtained by HD and MC simulations.

II. THE ANOMALOUS SIMULATION EFFECT

The energy balance equation represents the main difference between the HD and the DD transport model. The benefit of the increased computational effort of solving an additional equation with the HD model is that the carrier temperature can differ from the lattice temperature. Since the diffusion of the carriers is proportional to their temperature, the diffusion can be significantly higher with the HD transport model. Fig. 2 clearly shows the enhanced vertical diffusion of electrons as compared with the DD result in Fig. 3.

When simulating SOI MOSFETs, this increased diffusion has a strong impact on the body potential because the hot electrons

0018-9383/02$17.00 © 2002 IEEE

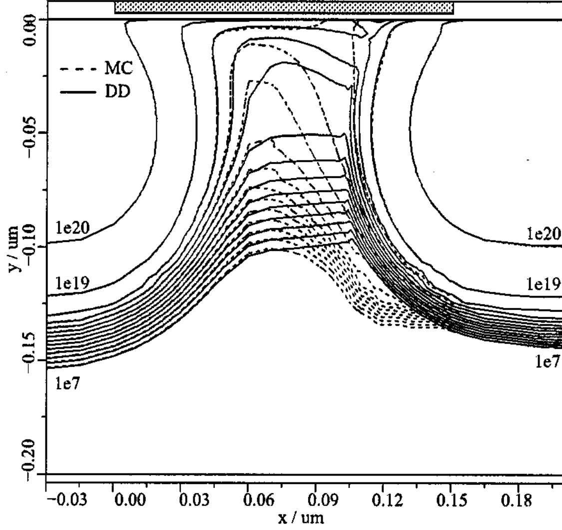

Fig. 3. Electron concentration in an SOI MOSFET obtained by DD and MC simulations.

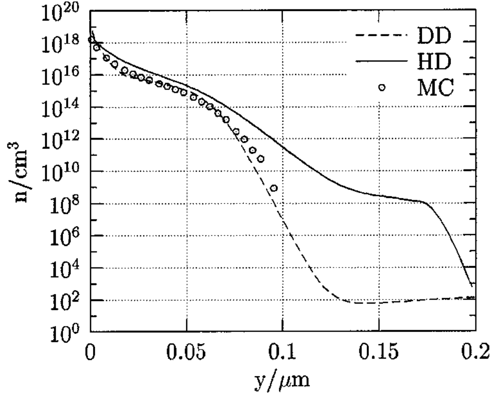

Fig. 4. Electron concentration in a MOSFET at a vertical cut located in the middle between source and drain.

of the pinch-off region have enough energy to overcome the energy barrier toward the floating body region and thus enter into the sea of holes. Some of these electrons in the floating body are collected by the drain-body and source-body junctions, but most recombine. The holes removed by recombination cause the body potential to drop. A steady state is obtained when the body potential reaches a value which biases the junctions enough in reverse direction so that thermal generation of holes in the junctions can compensate this recombination process. The decrease in the output characteristics is then connected to the drop of the body potential via the body-effect. Note that this effect can only be observed in partially depleted devices. It disappears gradually when changing the device parameters so as to make the device fully depleted.

III. Modified Hydrodynamic Equations

In MC simulations, the spreading of hot carriers away from the interface is much less pronounced than in HD simulations (Fig. 4). If we assume that the Boltzmann equation does not predict the hot-carrier spreading and if the standard HD equations derived from the Boltzmann equation do so, the problem must be introduced by the assumptions made in the derivation of the HD model. As the most relevant assumptions, we consider the approximation of tensor quantities by scalars and the closure of the hierarchy of moment equations.

To relax these assumptions, we reconsider the derivation of the HD equation set from the Boltzmann equation which reads

$$\frac{\partial f}{\partial t} + \mathbf{v} \cdot \nabla_r f + s_b q \mathbf{E} \cdot \nabla_p f = Q(f). \tag{1}$$

Here, f denotes the distribution function, $\mathbf{v}$ the group velocity, s_b the sign of the carrier charge, that is, -1 for electrons and $+1$ for holes, q denotes the elementary charge, $\mathbf{E}$ the electric field, and Q the collision operator.

Using the method of moments, the Boltzmann equation is integrated in $\mathbf{k}$-space against the following weight functions ϕ_j

$$\begin{aligned} \phi_0 &= 1 \quad \boldsymbol{\phi}_1 = \hbar \mathbf{k} \\ \phi_2 &= \mathcal{E} \quad \boldsymbol{\phi}_3 = \mathbf{v}\mathcal{E}. \end{aligned}$$

The weight functions are scalars for even orders and vectors for odd orders. A single parabolic band is assumed, $\mathcal{E} = \hbar^2 \mathbf{k}^2 / 2m$. To express moments of the scattering operator Q the macroscopic relaxation time approximation is employed. This introduces relaxation times for momentum, energy, and energy flux, which are denoted by τ_m, $\tau_\mathcal{E}$ and τ_S, respectively. As a result, the following moment equations are obtained:

$$\phi_0 : \partial_t \langle 1 \rangle + \nabla \cdot \langle \mathbf{v} \rangle = 0 \tag{2}$$

$$\phi_2 : \partial_t \langle \mathcal{E} \rangle + \nabla \cdot \langle \mathbf{v}\mathcal{E} \rangle - s_b q \mathbf{E} \cdot \langle \mathbf{v} \rangle = - \frac{\langle \mathcal{E} \rangle - \langle \mathcal{E} \rangle_0}{\tau_\mathcal{E}} \tag{3}$$

$$\boldsymbol{\phi}_1 : \nabla \cdot \langle \mathbf{v} \otimes \mathbf{p} \rangle - s_b q \mathbf{E} \cdot \langle \widetilde{\delta} \rangle = - \frac{\langle \mathbf{p} \rangle}{\tau_m} \tag{4}$$

$$\boldsymbol{\phi}_3 : \nabla \cdot \langle \mathbf{v} \otimes \mathbf{v}\mathcal{E} \rangle - s_b q \mathbf{E} \cdot \left\langle \frac{\mathcal{E}}{m} \widetilde{\delta} + \mathbf{v} \otimes \mathbf{v} \right\rangle = - \frac{\langle \mathbf{v}\mathcal{E} \rangle}{\tau_S}. \tag{5}$$

The symbols used are $\langle \cdot \rangle = \int f(\mathbf{k}, \mathbf{r}, t) \cdot d^3k$ for the statistical average, $\otimes$ for the tensor product and $\widetilde{\delta}$ for the unity tensor.

The previous equation system is not closed as it contains more unknowns than equations. The four state variables commonly used are

$$n = \langle 1 \rangle \quad \frac{3}{2} k_B T_n = \frac{\langle \mathcal{E} \rangle}{\langle 1 \rangle} \tag{6}$$

$$\mathbf{J}_n = -q \langle \mathbf{v} \rangle \quad \mathbf{S}_n = \langle \mathbf{v}\mathcal{E} \rangle. \tag{7}$$

In order to capture more realistically the phenomenon of hot carrier diffusion we close the equation set by assuming an anisotropic temperature and a non-Maxwellian distribution function.

A. Anisotropic Maxwellian Distribution Function

Permitting different temperatures T_{xx}, T_{yy}, T_{zz} for the three spatial directions leads to an anisotropic Maxwellian distribution function of the form

$$f_M(\mathbf{k}) = n \prod_{i=1}^{3} \frac{1}{\sqrt{2\pi}} \frac{1}{\sigma_i} \exp\left(-\frac{k_i^2}{2\sigma_i^2} \right) \quad , i = x, y, z \tag{8}$$

with $\sigma_i^2 = mk_BT_{ii}/\hbar^2$. Asymmetry can be introduced by shifting the distribution by some wave vector $\mathbf{K}$

$$f_{\mathrm{SM}}(\mathbf{k}) = \frac{n}{(2\pi)^{3/2}} \prod_{i=1}^{3} \frac{1}{\sigma_i} \exp\left(-\frac{(k_i - K_i)^2}{2\sigma_i^2}\right). \tag{9}$$

In the diffusion approximation, the displacement in momentum is assumed to be much smaller than the thermal momentum, that is $K_i \ll \sigma_i$, such that a linear expansion of the shifted Maxwellian distribution with respect to K_i/σ_i is justified

$$f(\mathbf{k}) \approx f_M(\mathbf{k}) + \left(\frac{k_xK_x}{\sigma_x^2} + \frac{k_yK_y}{\sigma_y^2} + \frac{k_zK_z}{\sigma_z^2}\right) f_M(\mathbf{k}). \tag{10}$$

Evaluating the statistical averages of the tensor products in (2)–(5) using the distribution function (10) results in diagonal tensors. The resulting flux equations read

$$\mathbf{J}_n = -\frac{q}{m}\langle p\rangle = \frac{q\tau_m}{m}\left(\nabla\cdot\left(k_Bn\widetilde{T}\right) + q\mathbf{E}n\right) \tag{11}$$

$$\mathbf{S}_n = -\frac{\tau_S k_B^2}{2m}\left(\nabla\cdot\left(n\left(3T_n + 2\widetilde{T}\right)\widetilde{T}\right) + \frac{q}{k_B}n\mathbf{E}\left(3T_n + 2\widetilde{T}\right)\right) \tag{12}$$

where the temperature tensor is denoted by $\widetilde{T} = \mathrm{diag}(T_{xx}, T_{yy}, T_{zz})$. For the here considered parabolic bands it can be easily shown that

$$T_n = \frac{1}{3}\left(T_{xx} + T_{yy} + T_{zz}\right). \tag{13}$$

The carrier continuity equation and the energy balance equation are not affected by the anisotropy

$$\nabla\cdot\mathbf{J}_n = q\partial_t n \tag{14}$$

$$\nabla\cdot\mathbf{S}_n = -\frac{3}{2}k_B\partial_t\left(nT_n\right) + \mathbf{E}\cdot\mathbf{J}_n - \frac{3}{2}k_Bn\frac{T_n - T_L}{\tau_{\mathcal{E}}}. \tag{15}$$

B. Isotropic Non-Maxwellian Distribution Function

As a second effect, we investigate the influence of the shape of the distribution function on the HD transport model. The starting point is a generic, non-Maxwellian distribution $f_{\mathrm{NM}}(\mathcal{E}(\mathbf{k}))$. The diffusion approximation requires linearization for small displacement vectors $\mathbf{K}$

$$f_{\mathrm{NM}}(\mathcal{E}(\mathbf{k}-\mathbf{K})) \simeq f_{\mathrm{NM}}(\mathcal{E}(\mathbf{k})) - \frac{\partial f_{\mathrm{NM}}}{\partial\mathcal{E}}\mathbf{v}\cdot\hbar\mathbf{K}. \tag{16}$$

The two terms on the right-hand side represent the distribution function's symmetric and antisymmetric parts, respectively. Note that all tensor products in (4) and (5) are even functions of $\mathbf{k}$ and hence their statistical average will depend only on the symmetric part f_{NM}. From the symmetries of $\mathcal{E}(\mathbf{k})$, such as $\mathcal{E}(-k_x,k_y,k_z) = \mathcal{E}(k_x,k_y,k_z)$, it follows that the off-diagonal elements of the statistical averages vanish. Without the linearization performed within the diffusion approximation (16) the symmetric part of the distribution function would be different and the off-diagonal elements would be nonzero. Because of invariance of $\mathcal{E}(\mathbf{k})$ to permutations such as $\mathcal{E}(k_x,k_y,k_z) = \mathcal{E}(k_y,k_x,k_z)$ all diagonal elements are equal. Therefore, the flux equations (4) and (5) simplify to

$$\mathbf{J}_n = \mu_nk_B\left(\nabla\left(nT_n\right) + \frac{q}{k_B}\mathbf{E}n\right) \tag{17}$$

$$\mathbf{S}_n = -\tau_S\left(\frac{1}{3}\nabla\left\langle v^2\mathcal{E}\right\rangle + \frac{5}{2}\frac{qk_B}{m}\mathbf{E}nT_n\right). \tag{18}$$

The moment of fourth order $\langle v^2\mathcal{E}\rangle$ remains as an unknown. To close the equation set this moment needs to be approximated as a function of the lower order moments. For a Maxwellian distribution f_M and parabolic bands the following, widely used closure is obtained

$$\left\langle v^2\mathcal{E}\right\rangle_M = \frac{15}{2}\frac{k_B^2}{m}nT_n^2. \tag{19}$$

In case of a non-Maxwellian distribution f_{NM}, we use the normalized moment of fourth order

$$\beta_n = \frac{\left\langle v^2\mathcal{E}\right\rangle_{\mathrm{NM}}}{\left\langle v^2\mathcal{E}\right\rangle_M} \tag{20}$$

which gives the energy flux equation of the form

$$\mathbf{S}_n = -\frac{5}{2}\frac{k_B}{q}\mu_S\left(k_B\nabla\left(nT_n^2\beta_n\right) + q\mathbf{E}nT_n\right) \tag{21}$$

with a mobility defined by $\mu_S = q\tau_S/m$.

C. Anisotropic Non-Maxwellian Distribution Function

Now the changes in the flux equations resulting from the anisotropy and the non-Maxwellian shape of the distribution function are combined. Considering a generic space direction characterized by the unit vector $\mathbf{e}_\xi$ we obtain

$$J_{n,\xi} = \mu_n\left(k_B\nabla_\xi\left(nT_{\xi\xi}\right) + qE_\xi n\right) \tag{22}$$

$$S_{n,\xi} = -\frac{5}{2}\frac{k_B}{q}\mu_S\left(k_B\nabla_\xi\left(n\beta_nT_{\xi\xi}\Theta\right) + qE_\xi n\Theta\right) \tag{23}$$

$$\Theta = \frac{3T_n + 2T_{\xi\xi}}{5}. \tag{24}$$

The carrier temperature T_n defined by (6) is a measure of average carrier energy. The diagonal component of the temperature tensor is given by $k_BT_{\xi\xi} = \langle v_\xi p_\xi\rangle$. Off-diagonal components are neglected. β_n is the normalized moment of fourth order defined by (20). The solution variable is still the carrier temperature T_n, whereas the tensor components and the fourth-order moment are modeled empirically as functions of T_n.

By assuming an isotropic Maxwellian distribution, which results in $T_{\xi\xi} = T_n$ and $\beta_n = 1$, the conventional HD model is obtained.

D. Temperature Tensor Modeling

The empirical model for the temperature tensor distinguishes between directions parallel (x) and normal (y) to the current density

$$T_{xx} = \gamma_xT_n, \qquad T_{yy} = \gamma_yT_n \tag{25}$$

$$\gamma_\nu\left(T_n\right) = \gamma_{0\nu} + \left(1 - \gamma_{0\nu}\right)\exp\left(-\left(\frac{T_n - T_L}{T_{\mathrm{ref},\gamma}}\right)^2\right), \nu = x, y. \tag{26}$$

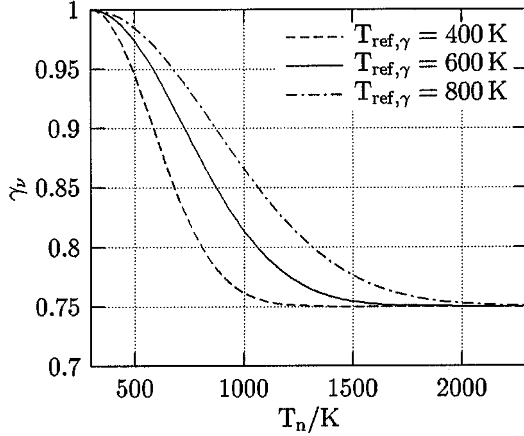

Fig. 5. Shape of the function used to model γ and β.

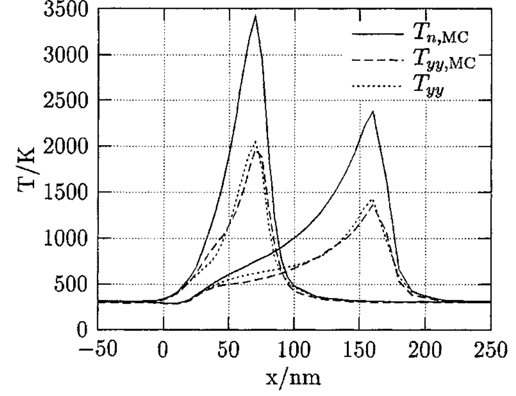

Fig. 6. MC simulation of a 90-nm and a 180-nm MOSFET showing the y-component of the temperature at the surface compared to the temperature $T_{n,\mathrm{MC}}$ from the mean energy. The analytical T_{yy} uses $\gamma_{0\nu} = 0.6$.

The anisotropy functions $\gamma_\nu(T_n)$ give 1 for $T_n = T_L$ and an asymptotic value $\gamma_{0\nu}$ for large T_n (Fig. 5), ensuring that only for sufficiently hot carriers the distribution becomes anisotropic, whereas the equilibrium distribution stays isotropic (Fig. 6). With respect to numerical stability the transition should not be too steep. $T_{\mathrm{ref},\gamma} = 600$ K appeared to be appropriate. The diagonal temperature for a generic direction $\mathbf{e}_\xi = (\cos\varphi, \sin\varphi)$ is obtained from the average $\langle \mathbf{v}\cdot\mathbf{e}_\xi \mathbf{p}\cdot\mathbf{e}_\xi\rangle$ after neglecting the off-diagonal terms as

$$T_{\xi\xi} = T_{xx}\cos^2\varphi + T_{yy}\sin^2\varphi. \tag{27}$$

E. Closure Relation Modeling

Another effect observed in MC simulations is that in most parts of the device the high energy tail is less populated than that of a Maxwellian distribution. Such underpopulation of the energy tail is reflected by a value of $\beta_n < 1$. Aiming at a model only for the region where $\beta_n < 1$ (see Fig. 7), a simple expression for β_n has been assumed

$$\beta_n(T_n) = \beta_0 + (1-\beta_0)\exp\left(-\left(\frac{T_n - T_L}{T_{\mathrm{ref},\beta}}\right)^2\right). \tag{28}$$

The functional form of $\beta_n(T_n)$ is identical to the one of the anisotropy function $\gamma_\nu(T_n)$ [cf. (26)]. Again, this expression ensures that only for sufficiently large T_n the distribution deviates from the Maxwellian shape.

The condition $\beta_n > 1$ characterizes an overpopulation of the energy tail as compared to a Maxwellian distribution. This situation occurs where channel hot carriers arrive at the drain region and a mixture of hot and cold carriers exists. We assume that the hot subpopulation existing in this transition region has only little influence on the hot-carrier diffusion into the floating body.

IV. Results

The modified flux equations have been implemented in MINIMOS-NT using a straight forward extension of the Scharfetter-Gummel discretization scheme (Appendix A). Numerical stability does not degrade as compared to standard HD simulations.

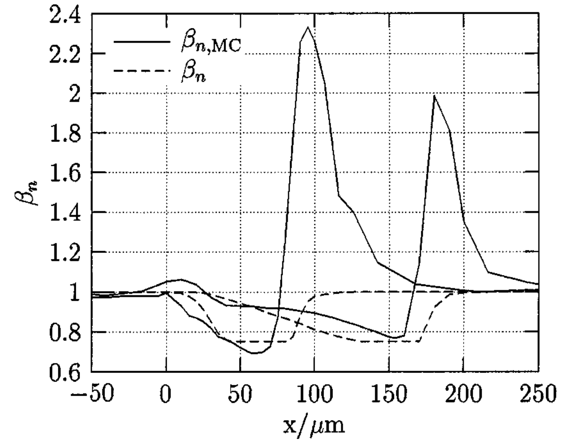

Fig. 7. MC simulation of a 90-nm and a 180-nm MOSFET showing the normalized moment of fourth order $\beta_{n,\mathrm{MC}}$ at the surface compared to the analytical β_n with $\beta_0 = 0.75$.

Parameter values were estimated from MC results obtained by simulating MOS transistors using the MC code described in [6].

As a first example simulations were performed on a device with an assumed effective gate-length of 130 nm, a gate-oxide thickness of 3 nm, and a silicon-film thickness of 200 nm. With a p-doping of $N_A = 7.5\cdot 10^{17}$ cm^{-3} the device is partially depleted. The Gaussian-shaped n-doping under the electrodes has a maximum of $N_D = 6\cdot 10^{20}$ cm^{-3}.

Fig. 6 indicates that $\gamma_{0y} = 0.6$ is a realistic value for the anisotropy parameter. Fig. 8 shows the influence of γ_{0y} on the output characteristics. By accounting for a reduced vertical temperature it is possible to reduce the spurious current decrease, but only to a certain degree and by assuming a fairly large anisotropy. MC simulations yield values close to $\beta_0 = 0.75$ for the non-Maxwellian parameter in the channel region (Fig. 7). This parameter shows only a weak dependence on doping and applied voltage.

By combining the modifications for an anisotropic temperature and a non-Maxwellian closure relation the artificial current decrease gets eliminated (Fig. 9). Parameter values roughly estimated from MC simulations can be used, e.g., $\gamma_{0y} = 0.75$ and $\beta_0 = 0.75$. In the parameter range where the current drop is

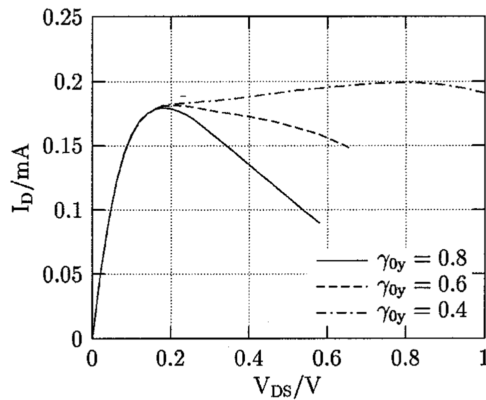

Fig. 8. Output characteristics of the SOI obtained by anisotropic HD simulations without closure modification ($\beta_0 = 1$).

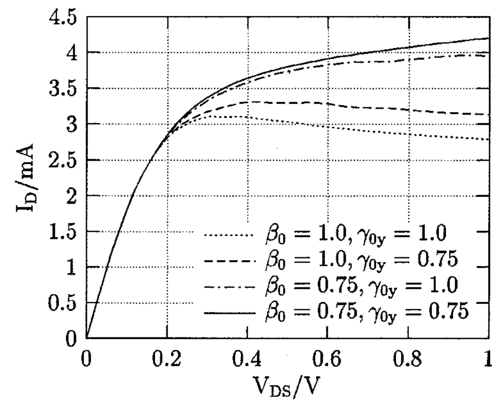

Fig. 10. Output characteristics of the "well-tempered" SOI at $V_{GS} = 1$ V.

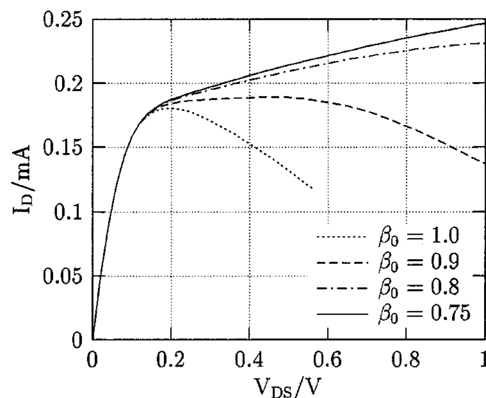

Fig. 9. Output characteristics of an SOI-MOSFET with analytical doping profile assuming an anisotropic temperature ($\gamma_{0y} = 0.75$) and a modified closure relation at $V_{GS} = 1$ V.

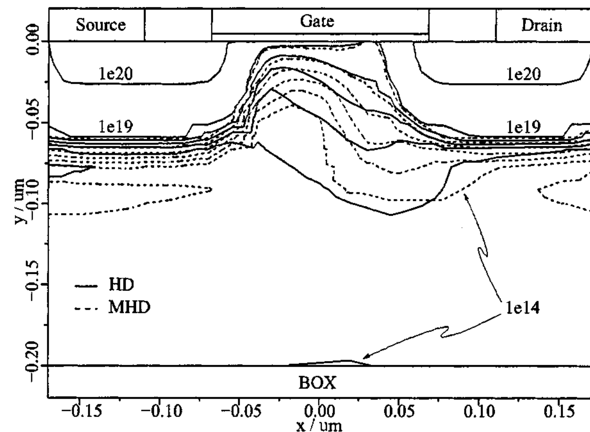

Fig. 11. Electron concentration in the "well-tempered" SOI obtained by a standard HD and a modified HD simulation.

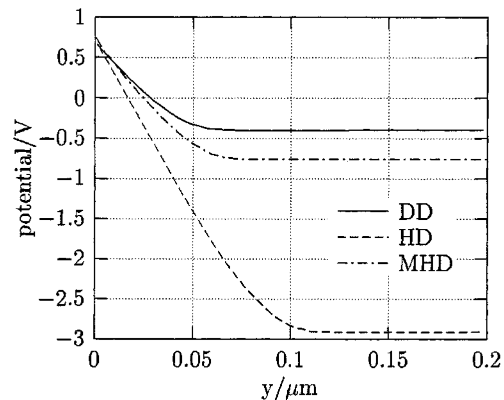

Fig. 12. Vertical potential distribution in the "well-tempered" SOI obtained by DD, HD, and modified HD simulations.

eliminated the output characteristics are found to be rather insensitive to the parameter values.

When the modified model is applied to a body-contacted MOSFET, the difference in the output characteristic is only marginal compared to the standard hydrodynamic transport model. For example, using the values $\gamma_{0y} = 0.6$ and $\beta_0 = 0.75$ leads to a maximum deviation of about 0.3% in the drain current within the bias range.

To verify the modified hydrodynamic transport model, a second device has been investigated. Basically this SOI has been modeled after the 90-nm "well-tempered" MOSFET [7] using the doping profiles available online, including the super steep retrograde (SSR) channel doping and source/drain halo. To achieve a partially depleted device a substrate doping of $N_A = 7.5 \cdot 10^{17}$ cm^{-3} has been assumed and the substrate thickness has been limited to 200 nm.

By using the standard HD transport model the drop in the drain current is also present in this device ($\beta_0 = 1.0$, $\gamma_{0y} = 1.0$ in Fig. 10). Applying the modified model using the same parameters as before the output characteristics obtain their normal shape. The different order of magnitude of the drain currents seen with Device 1 and Device 2 mainly stems from the rather high threshold voltage of Device 1.

The difference in the electron concentration is shown in Fig. 11. In the case of the standard HD model, the spreading of the hot electrons is much more pronounced than with the modified one.

By looking at the potential in the device at a vertical cut located in the middle between source and drain (Fig. 12), the difference between the standard HD model and the modified one is also clearly visible.

It appeared that in contrast to MOS devices the grid in the floating body region plays a crucial role to the stability of the simulation and the quality of the result. This is due to the fact

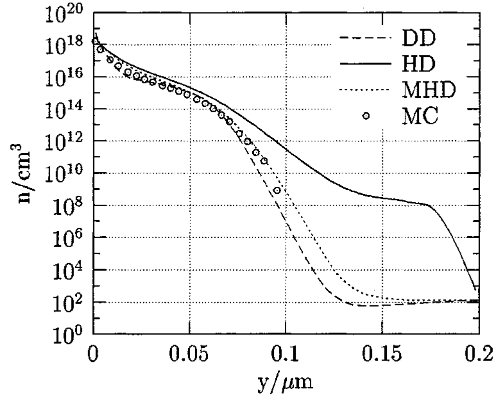

Fig. 13. Comparison of the electron concentration in a MOSFET at a vertical cut located in the middle between source and drain obtained by simulations using DD-, HD-, MC-, and the modified HD model.

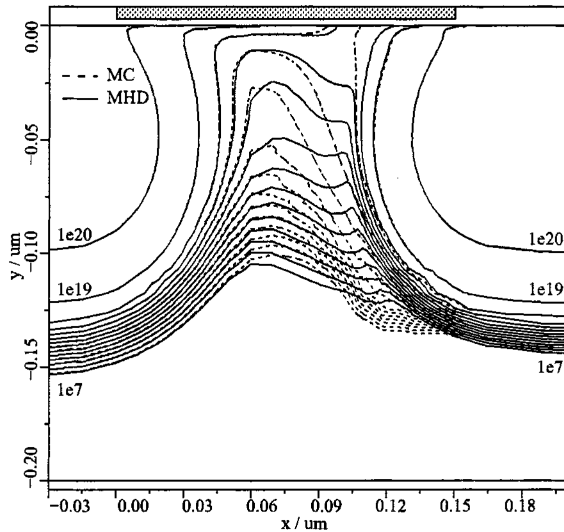

Fig. 14. Electron concentration in a MOSFET obtained by simulations using the modified HD model compared to MC data.

that the drain current is very sensitive to the location of the potential drop in the floating region.

The simulations that lead to Fig. 4 were repeated with the modified HD transport model and the result obtained is shown in Fig. 13. As can be seen, good agreement with MC data is obtained (see Fig. 14). This confirms that the correction of the SOI output characteristics obtained with the modified model is based on a corrected behavior of the electron distribution in the bulk.

V. Conclusion

Standard HD simulations of SOI MOSFET give anomalous output characteristics. To solve this problem, an improved HD transport model has been developed. By including two distinct modifications, namely, an anisotropic carrier temperature and a modified closure relation, the spurious diffusion of hot electrons in the vertical direction has been sufficiently reduced. The improved hydrodynamic transport model has successfully been used to simulate different SOI devices.

Appendix
Flux Discretization

For the discretization of the flux equations (22) and (23), we make use of the observation that both fluxes $J_{n,\xi}$ and $S_{n,\xi}$ can be written in a general form as

$$-\frac{\Phi}{C_\Phi} = \frac{d}{d\xi}\left(\nu T_\Phi\right) - s_b \frac{q}{k_B} E\nu \tag{29}$$

with

$$\begin{aligned} \Phi &= J_{n,\xi}: \quad \nu = n \\ T_\Phi &= T_{\xi\xi} \quad C_\Phi = s_b k_B \mu_n \end{aligned} \tag{30}$$

$$\begin{aligned} \Phi &= S_{n,\xi}: \quad \nu = n\frac{3T_n + 2T_{\xi\xi}}{5} \\ T_\Phi &= T_{\xi\xi}\beta_n, \quad C_\Phi = \frac{5}{2}\frac{k_B^2}{q}\mu_S. \end{aligned} \tag{31}$$

Assuming that the projected flux between two grid points is constant and that the temperature associated to each flux T_Φ varies linearly on the edge gives the following Scharfetter-Gummel-type discretization form of the flux

$$\Phi = -\frac{C_\Phi}{\Delta\xi}\frac{\Delta T_\Phi}{\ln\left(\frac{T_{\Phi j}}{T_{\Phi i}}\right)}\left(\nu_j \mathcal{B}(Y_\Phi) - \nu_i \mathcal{B}(-Y_\Phi)\right) \tag{32}$$

$$Y_\Phi = -\frac{\ln\left(\frac{T_{\Phi j}}{T_{\Phi i}}\right)}{\Delta T_\Phi}\left(s_b\frac{q}{k_B}\Delta\psi + \Delta T_\Phi\right) \tag{33}$$

where $\mathcal{B}(\cdot)$ is the Bernoulli function.

References

[1] T. Simlinger, H. Brech, T. Grave, and S. Selberherr, "Simulation of submicron double-heterojunction high electron mobility transistors with MINIMOS-NT," *IEEE Trans. Electron Devices*, vol. 44, pp. 700–707, May 1997.

[2] *DESSIS-ISE Users Manual, Release 6*, ISE Integr. Syst. Eng. AG, Zürich, Switzerland, 1999.

[3] M. Gritsch, H. Kosina, T. Grasser, and S. Selberherr, "Influence of generation/recombination effects in simulations of partially depleted SOI MOSFETs," *Solid-State Electron.*, vol. 45, no. 4, pp. 621–627, 2001.

[4] ——, "A simulation study of partially depleted SOI MOSFETs," *Silicon-on-Insulator Technol. Devices X*, pp. 181–186, Mar. 2001.

[5] J. L. Egley, B. Polsky, B. Min, E. Lyumkis, O. Penzin, and M. Foisy, "SOI related simulation challenges with moment based BTE solvers," *Simulation Semicond. Processes Devices*, pp. 241–244, Sept. 2000.

[6] H. Kosina and S. Selberherr, "A hybrid device simulator that combines Monte Carlo and drift-diffusion analysis," *IEEE Trans. Computer-Aided Design*, vol. 13, pp. 201–210, Feb. 1994.

[7] D. A. Antoniadis, I. J. Djomehri, K. M. Jackson, and S. Miller, "Well-tempered," *Bulk-Si NMOSFET Device Home Page*, Nov. 2001, http://www.-mtl.edu/Well/.

Markus Gritsch was born in Zams, Austria, in 1974. He received the Dipl.Ing. degree in electrical engineering from the Technische Universität Wien, Vienna, Austria, in 1999. He has been pursuing the Ph.D. degree at the Institut für Mikroelektronik, Technische Universität Wien, Vienna, since May 1999.

His scientific interests include circuit and device simulation, device modeling, and physical and software aspects in general.

Hans Kosina (S'89–M'93) received the Dipl.Ing. degree in electrical engineering and the Ph.D. degree in technical sciences from the Technische Universität Wien, Vienna, Austria, in 1987 and 1992, respectively.

In 1988, he joined the Institut für Mikroelektronik, Technische Universität Wien, where he is currently employed as an Associate Professor. In March 1998, he received the "venia docendi" on Microelectronics. His current research topics include modeling of carrier transport and quantum effects in semiconductor devices, development of novel Monte-Carlo algorithms, and computer-aided engineering in ULSI-technology.

Tibor Grasser was born in Vienna, Austria, in 1970. He studied communications engineering and received the Diploming. and the Ph.D. degree in technical sciences from the Technische Universität Wien, Vienna, in 1995 and 1999, respectively.

He joined the Institut für Mikroelektronik, Technische Universität Wien, in 1996, where he is currently an Associate Professor. In 2002, he received the "venia docendi" on Microelectronics. Since 1997, he has Headed the MINIMOS-NT Development Group, working on the successor to the highly successful MINIMOS Program. From October to December 1997, he was with Hitachi Ltd., Tokyo, Japan, as a Visiting Research Engineer. In Summer 2001, he was a Visiting Researcher with the Alpha Development Group, Compaq Computer Corporation, Shrewsbury, MA. His current scientific interests include circuit and device simulation, device modeling, and physical and software aspects in general.

Siegfried Selberherr (M'79–SM'84–F'93) was born in Klosterneuburg, Austria, in 1955. He received received the Diploming. degree in electrical engineering and the Ph.D. degree in technical sciences from the Technische Universität Wien, Vienna, Austria, in 1978 and 1981, respectively.

He has held the "venia docendi" on Computer-Aided Design since 1984. Since 1988, he has been the Head of the Institut für Mikoelektronik, Technische Universität Wien, and since 1999, he has been Dean of the Fakultät für Elektrotechnik und Informationstechnik. His current topics are modeling and simulation of problems for microelectronics engineering.